Smart Structures and Systems, *Vol. 14, No. 3 (2014) 267-284*
DOI: http://dx.doi.org/10.12989/sss.2014.14.3.267

Electromechanical analysis of 2-2 cement-based piezoelectric transducers in series electrically

Jianjun Wang and Zhifei Shi*

School of Civil Engineering, Beijing Jiaotong University, Beijing 100044, P. R. China

(Received December 13, 2012, Revised June 20, 2013, Accepted June 29, 2013)

Abstract. This paper aims to present the analytical solutions of 2-2 cement based piezoelectric transducers in series electrically based on the theory of piezo-elastic dynamics. The solutions of two different kinds of 2-2 cement based piezoelectric transducers under external harmonic load are obtained by using the displacement method. The effects of electrical connection of piezoelectric layers, loading frequency, thickness and distance of piezoelectric layers on the characteristics of the transducers are discussed. Comparisons with other related experimental investigations are also given, and good agreement is found. The proposed 2-2 cement based piezoelectric transducers have a great potential application in monitoring structural health in civil engineering and capturing mechanical energy or monitoring train-running safety in railway system and traffic safety in road system.

Keywords: 2-2 cement composite; piezoelectric transducer; actuator; series; dynamic behavior

1. Introduction

Nowadays, health monitoring of structures have been getting more and more attention (Aizawa *et al.* 1998, Huston *et al.* 1994). Li *et al.* (2004) presented an overview of current research and development in the field of structural health monitoring with civil engineering applications. Song *et al.* (2006) presented the concept of intelligent reinforced concrete structures (IRCS) and extended it to structural health monitoring in civil engineering. Additionally, they developed embedded piezoceramic transducers (Song *et al.* 2007) and a piezoceramic-based wireless sensor network (Li *et al.* 2010) used in concrete structural health monitoring. Jang *et al.* (2010) and Jang *et al.* (2012) used the wireless smart sensors to monitor the health of a cable-stayed bridge and a historic steel bridge, respectively. As one fundamental element of a health monitoring system and an active vibration control system, sensors and actuators should be durable, inexpensive, compatible with the host structure and preferentially active. Many achievements have been obtained on the performances of various traditional piezoelectric smart devices. Shi and his co-workers studied the mechanical and electrical behavior of several piezoelectric actuators, including multi-layer piezoelectric beams, piezoelectric curved actuators and functionally graded piezoelectric beams (Li and Shi 2009, Xiang and Shi 2008, 2009, Yao and Shi 2011, Zhang and Shi 2006). Huang *et al.* (2007, 2008) deduced piezo-elasticity solutions for functionally graded

*Corresponding author, Professor, E-mail: zfshi178@sohu.com

http://www.techno-press.org/?journal=sss&subpage=8 ISSN: 1738-1584 (Print), 1738-1991 (Online)

piezoelectric beams under the plane stress condition. Lim *et al.* (2001) and Bian *et al.* (2006) presented a state space formulation to study the parallel piezoelectric bimorph and the functionally graded beam actuators and sensors, respectively. Yang and Xiang (2007) investigated the static bending, free vibration and dynamic response of monomorph, bimorph and multimorph actuators made of functionally graded piezoelectric materials. Besides, Yang *et al.* (2004) also analyzed the non-linear bending behavior of functionally graded plates with piezoelectric actuators. In order to improve the output displacements of the functionally graded piezoelectric bimorph type actuators, Carbonari *et al.* (2006, 2007) presented topology optimization formulation to find the optimum gradation and polarization sign variation in piezoceramic domains.

Smart materials and structures have been gradually infiltrating into the field of civil engineering. In order to overcome the problem that piezoelectric materials have poor compatibility with concrete, researchers have given their attentions to the fabrication and use of cement-based piezoelectric composites in civil engineering, such as 0-3, 1-3, 2-2, sandwich cement based piezoelectric composites (Chaipanich 2007, Li *et al.* 2006, Li *et al.* 2007, Xu *et al.* 2009, 2011). In these piezoelectric composites, 2-2 cement based piezoelectric composites have both desirable sensor effects and actuator effects (Dong and Li 2005, Li *et al.* 2001, Zhang *et al.* 2002). However, most of works focused on the fabrication and detection for cement-based piezoelectric composites. Theoretical investigations on the behavior of these piezoelectric composites, especially on the dynamic behavior are very limited. Shi and his co-workers have been focused on presenting the exact theoretical analysis of these piezoelectric composites (Han and Shi 2011, Han *et al.* 2011, Han and Shi 2012, Shi and Wang 2013, Zhang and Shi 2011). Based on our previous works, the properties of 2-2 cement-based piezoelectric transducers in series electrically are further analyzed based on the theory of piezo-elastic dynamics. In Section 2, the basic equations for 2-2 cement based piezoelectric transducers are summarized. In Section 3, two different kinds of 2-2 cement based piezoelectric transducers under external load are considered and the analytical solutions are obtained by using the displacement method. In Section 4, comparisons with other related experimental investigations are conducted and good agreement is found. In addition, the effects of electrical connection of piezoelectric layers, loading frequency, thickness and distance of piezoelectric layers on the characteristics of the transducers are also discussed.

2. Basic equations

Two kinds of 2-2 cement-based piezoelectric transducers as shown in Figs. 1 and 2 are considered. Both transducers consist of $N+1$ cement layers and N piezoelectric layers, and they are arranged alternatively. The thicknesses of the cement layer i and the piezoelectric layer i are determined by $(h_{2i-1}-h_{2i-2})$ and $(h_{2i}-h_{2i-1})$, respectively. The thickness of every layer may be different. All of the piezoelectric layers are polarized along its thickness direction. Besides, the piezoelectric coefficient will be defined as plus or minus depending on the polarization direction in the positive z-axis or negative z-axis (Xiang and Shi 2008). The governing equations for the piezoelectric layer i and the cement layer i have been listed in previous article (Shi and Wang 2013). In the present paper, the following harmonic external loads are considered

$$\begin{cases} V(t)=V_0e^{j\omega t},\ q(t)=q_0e^{j\omega t} & \text{(for case 1)} \\ q(t)=q_0e^{j\omega t} & \text{(for case 2)} \end{cases} \tag{1}$$

where q_0 and V_0 are the external load amplitude, $j=\sqrt{-1}$, $\omega=2\pi f$ is the circular frequency, t is the time.

For harmonic steady vibration, the solutions with the following forms can be assumed

$$(u_{Pi},\sigma_{zPi},\phi_i,D_{zi})=[u_{Pi}(z),\sigma_{zPi}(z),\phi_i(z),D_{zi}(z)]e^{j\omega t} \quad \text{(for piezoelectric layer } i\text{)} \tag{2}$$

$$(u_{Ci},\sigma_{zCi})=[u_{Ci}(z),\sigma_{zCi}(z)]e^{j\omega t} \quad \text{(for cement layer } i\text{)} \tag{3}$$

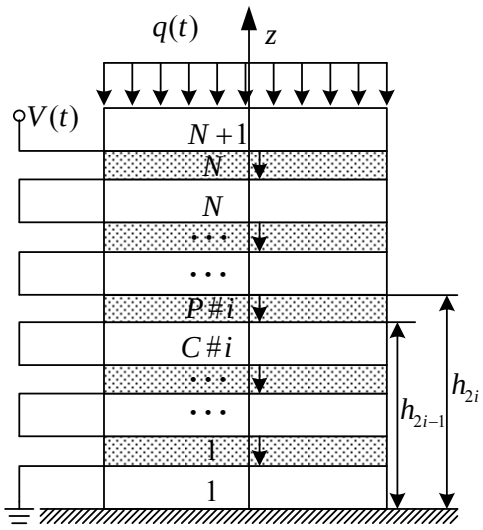

Fig. 1 Schematic of 2-2 cement based piezoelectric transducer under a voltage and a uniformly distributed load (case 1)

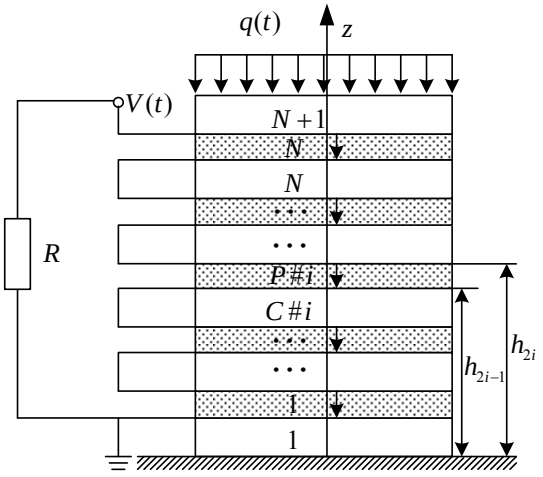

Fig. 2 Schematic of 2-2 cement based piezoelectric transducer under a uniformly distributed load (case 2)

where σ_{zPi} and u_{Pi} are the stress and displacement components of the piezoelectric material along the z direction, respectively; D_{zi} and ϕ_i represent the electric displacement and electric potential in the same direction, respectively.

Furthermore, the detailed expressions of $u_{Pi}(z)$, $\sigma_{zPi}(z)$, $\phi_i(z)$, $D_{zi}(z)$, $u_{Ci}(z)$ and $\sigma_{zCi}(z)$ can be derived (Shi and Wang 2013)

$$\begin{cases} u_{Pi}(z) = A_{Pi}\sin k_{Pi}z + B_{Pi}\cos k_{Pi}z \\ \sigma_{zPi}(z) = p_{Pi}(A_{Pi}\cos k_{Pi}z - B_{Pi}\sin k_{Pi}z) + \dfrac{e_{33i}^2}{\kappa_{33i}^{\varepsilon}}C_{1i} \\ \phi_i(z) = \dfrac{e_{33i}}{\kappa_{33i}^{\varepsilon}}(A_{Pi}\sin k_{Pi}z + B_{Pi}\cos k_{Pi}z + C_{1i}z + C_{0i}) \\ D_{zi}(z) = -e_{33i}C_{1i} \end{cases} \tag{4}$$

$$\begin{cases} u_{Ci}(z) = A_{Ci}\sin k_{Ci}z + B_{Ci}\cos k_{Ci}z \\ \sigma_{zCi}(z) = p_{Ci}(A_{Ci}\cos k_{Ci}z - B_{Ci}\sin k_{Ci}z) \end{cases} \tag{5}$$

where $k_{Pi}^2 = \dfrac{\rho_{Pi}\omega^2}{C_{33Pi} + e_{33i}^2/\kappa_{33i}^{\varepsilon}}$, $p_{Pi} = (C_{33Pi} + \dfrac{e_{33i}^2}{\kappa_{33i}^{\varepsilon}})k_{Pi}$, $k_{Ci}^2 = \dfrac{\rho_{Ci}\omega^2}{C_{33Ci}}$, $p_{Ci} = C_{33Ci}k_{Ci}$. The symbols A_{Pi}, B_{Pi}, C_{1i}, C_{0i}, A_{Ci} and B_{Ci} are constants to be determined by the boundary conditions and connecting conditions; $C_{33Pi} = \dfrac{1}{S_{33Pi}}$, $e_{33i} = \dfrac{d_{33i}}{S_{33Pi}}$ and $\kappa_{33i}^{\varepsilon} = \kappa_{33i}^{\sigma} - \dfrac{d_{33i}^2}{S_{33Pi}}$, or S_{33Pi}, d_{33i} and κ_{33i}^{σ} are the elastic coefficient, piezoelectric coefficient and permittivity coefficient; ρ_{Pi} is the density of the piezoelectric material; C_{33Ci} and ρ_{Ci} are the elastic coefficient and density of the cement material.

3. Analytical solutions for 2-2 cement based piezoelectric transducers

3.1 Piezoelectric transducer subjected to a voltage and a uniformly distributed load

Fig. 1 shows the case of 2-2 cement based piezoelectric transducer subjected to a voltage and a uniformly distributed load. It is assumed that the polarization directions of piezoelectric layers lie along the negative z-axis. In order to find the analytical solution in this case, the boundary conditions and connecting conditions are considered. The mechanical and electrical boundary conditions and continuous conditions can be written as follows, respectively

$$\begin{cases} u_{C1}\big|_{z=0} = 0 \\ \sigma_{zC(N+1)}\big|_{z=h_{2N+1}} = -q(t) \end{cases} \tag{6}$$

$$\begin{cases} \phi_1\big|_{z=h_1} = 0 \\ \phi_N\big|_{z=h_{2N}} = V(t) \end{cases} \tag{7}$$

$$\begin{cases} u_{Pi}\big|_{z=h_{2i-1}} = u_{Ci}\big|_{z=h_{2i-1}} \\ u_{Pi}\big|_{z=h_{2i}} = u_{C(i+1)}\big|_{z=h_{2i}} \\ \sigma_{zPi}\big|_{z=h_{2i-1}} = \sigma_{zCi}\big|_{z=h_{2i-1}} \\ \sigma_{zPi}\big|_{z=h_{2i}} = \sigma_{zC(i+1)}\big|_{z=h_{2i}} \\ \phi_i\big|_{z=h_{2i}} = \phi_{(i+1)}\big|_{z=h_{2i+1}} \\ D_{zi}\big|_{z=h_{2i}} = D_{z(i+1)}\big|_{z=h_{2i+1}} \end{cases} \tag{8}$$

Combining Eqs. $(5)_1$ and $(6)_1$, the constant B_{C1} in the first cement layer is

$$B_{C1} = 0 \tag{9}$$

Combining Eqs. $(4)_3$ and $(7)_1$, the constant C_{01} in the first piezoelectric layer is

$$C_{01} = -(A_{P1}\sin k_P h_1 + B_{P1}\cos k_P h_1 + C_{11} h_1) \tag{10}$$

Substituting Eqs. (2)-(5) into Eq. (8), the following equations are obtained

$$\begin{cases} A_{Pi}\sin k_P h_{2i-1} + B_{Pi}\cos k_P h_{2i-1} = A_{Ci}\sin k_C h_{2i-1} + B_{Ci}\cos k_C h_{2i-1} \\ A_{Pi}\sin k_P h_{2i} + B_{Pi}\cos k_P h_{2i} = A_{C(i+1)}\sin k_C h_{2i} + B_{C(i+1)}\cos k_C h_{2i} \\ p_P(A_{Pi}\cos k_P h_{2i-1} - B_{Pi}\sin k_P h_{2i-1}) + \dfrac{e_{33}^2}{\kappa_{33}^{\varepsilon}} C_{1i} = p_C(A_{Ci}\cos k_C h_{2i-1} - B_{Ci}\sin k_C h_{2i-1}) \\ p_P(A_{Pi}\cos k_P h_{2i} - B_{Pi}\sin k_P h_{2i}) + \dfrac{e_{33}^2}{\kappa_{33}^{\varepsilon}} C_{1i} = p_C(A_{C(i+1)}\cos k_C h_{2i} - B_{C(i+1)}\sin k_C h_{2i}) \end{cases} \tag{11a}$$

$$\begin{cases} A_{Pi}\sin k_P h_{2i} + B_{Pi}\cos k_P h_{2i} + C_{1i} h_{2i} + C_{0i} \\ = A_{P(i+1)}\sin k_P h_{2i+1} + B_{P(i+1)}\cos k_P h_{2i+1} + C_{1(i+1)} h_{2i+1} + C_{0(i+1)} \\ C_{1(i+1)} = C_{1i} \end{cases} \tag{11b}$$

By solving Eqs. (11(a)) and (11(b)), all the unknown constants A_{Ci}, B_{Ci}, A_{Pi}, B_{Pi}, C_{1i} and C_{0i} can be obtained, which are listed in (A.1), (A.2), (A.3) and (A.4) in **Appendix A**, respectively. Furthermore, all the unknown constants can be obtained after determining A_{C1} and C_{11}. Substituting Eqs. (A.1) and $(5)_2$ into Eq. $(6)_2$, Eqs. (A.2)-(A.4) and $(4)_3$ into Eq. $(7)_2$, A_{C1}

and C_{11} can be respectively determined to be

$$A_{C1} = \frac{d_{05}}{d_{06}} \tag{12}$$

$$C_{11} = -\frac{d_{06}q_0 + d_{01}d_{05}p_C}{d_{02}d_{06}p_C} \tag{13}$$

where

$$\begin{cases} d_{01} = \delta_{N+1}^{1}\cos k_C h_{2N+1} - \delta_{N+1}^{2}\sin k_C h_{2N+1} \\ d_{02} = \lambda_{N+1}^{1}\cos k_C h_{2N+1} - \lambda_{N+1}^{2}\sin k_C h_{2N+1} \\ d_{03} = \delta_N^3 \sin k_P h_{2N} + \delta_N^4 \cos k_P h_{2N} + \delta_N^8 \\ d_{04} = \lambda_N^3 \sin k_P h_{2N} + \lambda_N^4 \cos k_P h_{2N} + \lambda_N^8 + \alpha_N h_{2N} \end{cases} \tag{14}$$

$$\begin{cases} d_{05} = \dfrac{V_0 \kappa_{33}^{\varepsilon} d_{02} p_C - q_0 d_{04}\left|e_{33}\right|}{p_C\left|e_{33}\right|} \\ d_{06} = d_{01}d_{04} - d_{02}d_{03} \end{cases} \tag{15}$$

Now, all the mechanical and electrical solutions of case 1 have been obtained. For this case, the electrical admittance Y can be expressed as

$$Y = \frac{1}{Z} = \frac{I(t)}{V(t)} = \frac{I_0}{V_0} \tag{16}$$

where Z is the electrical impedance. The current $I(t)$ can be expressed as follow

$$I(t) = -\int_S \frac{dD_{zN}}{dt} dS = -j\omega S\left|e_{33}\right|\alpha_N C_{11} e^{j\omega t} = I_0 e^{j\omega t} \tag{17}$$

where $I_0 = -j\omega S\left|e_{33}\right|\alpha_N C_{11}$.

3.2 Piezoelectric transducer subjected to a uniformly distributed load

Fig. 2 shows the case of 2-2 cement based piezoelectric transducer subjected to a uniformly distributed load. For this case, the Eqs. (6)-(11) and (A.1)-(A.14) in case 1 are still valid, respectively. If the electrodes are closed by an electric circuit with a load resistor, the electrical boundary conditions in case 2 can be given as

$$V(t) = RI(t) \tag{18}$$

The current $I(t)$ can be expressed as follow

$$I(t) = \int_S \frac{dD_{zN}}{dt} dS = j\omega S\left|e_{33}\right|\alpha_N C_{11} e^{j\omega t} = I_0 e^{j\omega t} \tag{19}$$

where $I_0 = j\omega S|e_{33}|\alpha_N C_{11}$.

Thus

$$V_0 = RI_0 \tag{20}$$

Substituting Eqs. (A.1) and $(5)_2$ into Eq. $(6)_2$, Eqs. (A.2)-(A.4), $(4)_3$ and (20) into Eq. $(7)_2$, C_{11} and A_{C1} can be respectively determined to be

$$C_{11} = d_{07} q_0 \tag{21}$$

$$A_{C1} = -\frac{q_0(1 + d_{02} d_{07} p_C)}{d_{01} p_C} \tag{22}$$

where

$$d_{07} = \frac{d_{03}}{p_C(d_{06} + j\omega RS d_{01} \kappa_{33}^{\varepsilon})} \tag{23}$$

Now, all the mechanical and electrical solutions for case 2 have been obtained.

Furthermore, the above analytical solutions can be used to approximately calculate a pure piezoelectric stack once the thicknesses of every cement layer tend to be zero. Additionally, the electromechanical coupling factor of a smart system is defined by Mason (1950) as

$$k_d^2 = \frac{f_a^2 - f_r^2}{f_a^2} \tag{24}$$

where f_r and f_a are the resonance and anti-resonance frequencies, respectively. The average power in the generator model is defined as

$$P = \frac{|V_0|_{,rms}^2}{R} \tag{25}$$

where V_0 can be obtained from Eq. (20). The symbol rms is the root mean square.

4. Comparison and discussion

In the previous sections, the analytical solutions of the mechanical components and electric components of 2-2 cement based piezoelectric transducers have been obtained. In this section, the dynamic properties of the transducer are studied and compared with other investigations. The size of the transducer is taken as $25 \times 17 \times 40\,\text{mm}^3$. The number N and the total thickness of the transducer is 15 and 40 mm, respectively. The thickness of both the first cement layer and the $N+1$ cement layer is 10.8 mm. The thicknesses of other cement and piezoelectric layers are taken as $h_c = h_{2i-1} - h_{2i-2} = 1.1\,\text{mm}$ and $h_p = h_{2i} - h_{2i-1} = 0.2\,\text{mm}$, respectively. The piezoelectric layers and the cement layers are made of PZT-SH ceramic and hardened Portland cement paste,

respectively.

First, the present theoretical results are compared with Flint's experimental findings and the previous parallel model for case 1. In Flint's investigation (Flint *et al.* 1995), the thickness and number of layers of the stack is 0.5 mm and 182, respectively. In the present analysis, the piezoelectric wafer thickness and number of layers are respectively taken as 0.5 mm and 182 as well. The thickness and number of elastic cement layers is chosen as $0.5\,\mu m$ and 183, respectively. Its elastic modulus and density are 13.9 Gpa and 2000 kg/m^3, respectively. Figs. 3 and 4 give the magnitude and phase of the coupled impedance changing with the loading frequency, respectively. According to the electrical convention, the coupled impedance of series model should be N^2 times that of the parallel model when the frequency departs far from the resonance and anti-resonance frequencies. Figs. 3 and 4 show that the present theoretical results agree very well with the experimental findings and the previous work for both the magnitude and phase of the coupled impedance. For a transducer, resonance and anti-resonance are two important parameters. Using the present method, the resonance and anti-resonance frequencies of 2-2 cement based piezoelectric transducer in series electrically as shown in Fig. 3 can also be predicted very well. Keeping the total thickness as constant, the effect of the distance h_C between two adjacent piezoelectric layers on the resonance and anti-resonance frequencies of a 2-2 cement based piezoelectric transducer is plotted in Fig. 5. It indicates that both the resonance and anti-resonance frequencies of the series model are greater than those of the parallel model. For the parallel model, there exists only one maximum value in both resonance and anti-resonance curves, respectively. However, for the series model, only one maximum value appears in anti-resonance curve; in addition, the resonance frequency increases with the increase of the distance h_C. Fig. 6 gives the influence of the distance h_P between two adjacent cement layers on the resonance frequency. It is found that both the resonance and anti-resonance frequencies of the series model are greater than those of the parallel model. Two kinds of models have the same characteristics that there exists only one minimum value in both resonance and anti-resonance curves, respectively. Further, Figs. 7 and 8 show the effects of the thickness and distance of piezoelectric layers on the first electromechanical coupling factor. It is found that the electrical connection has a little effect on the first electromechanical coupling factor and a matching first electromechanical coupling factor can be designed by changing the distance h_C. In addition, the first electromechanical coupling factor increases with the increase of the distance h_P.

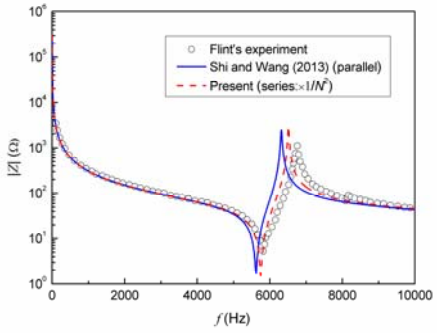

Fig. 3 Magnitude of coupled impedance versus the loading frequency

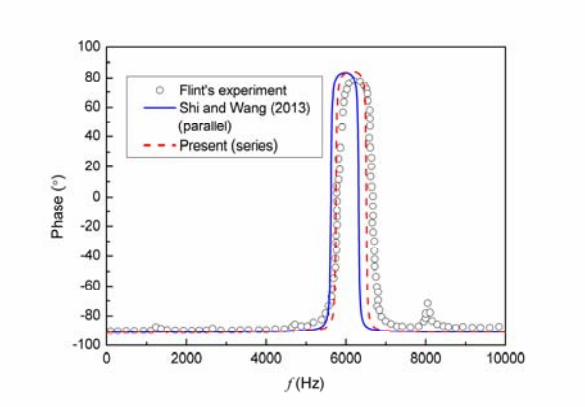

Fig. 4 Phase of coupled impedance versus the loading frequency

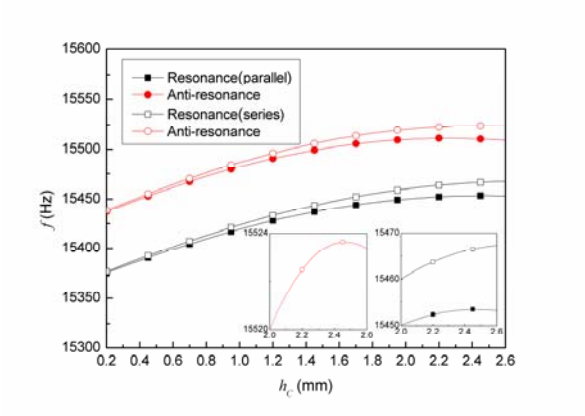

Fig. 5 Influence of the distance between two adjacent piezoelectric layers h_C on the resonance and anti-resonance frequencies

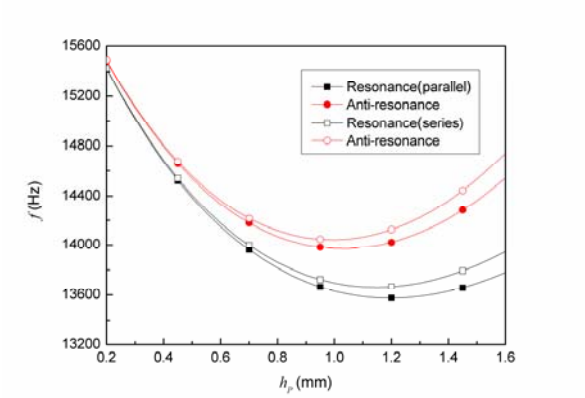

Fig. 6 Influence of the distance between two adjacent cement layers h_p on the resonance frequency

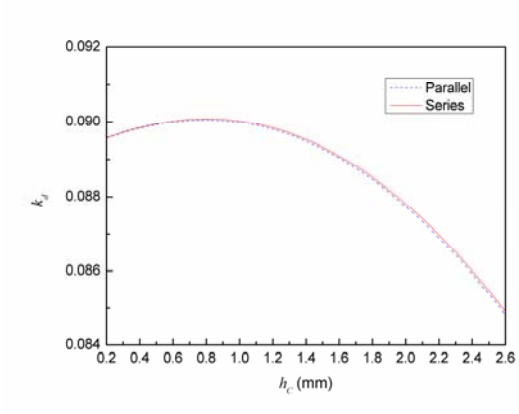

Fig. 7 The first electromechanical coupling factor changing with the distance between two adjacent piezoelectric layers h_C

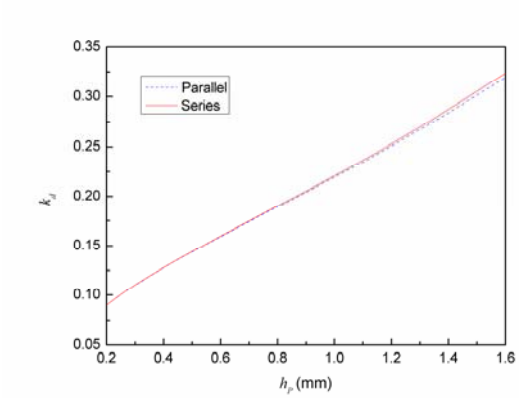

Fig. 8 The first electromechanical coupling factor changing with the distance between two adjacent cement layers h_P

Second, the present theoretical results are compared with Feenstra's experimental findings and the previous parallel model for case 2. Feenstra *et al.* conducted an experimental study on the energy harvest through a mechanically amplified piezoelectric stack (Feenstra *et al.* 2008). The stack consists of 130 layers and the total thickness and the cross section of the stack is 16 mm and 25 mm^2, respectively. In the present analysis, the thickness of every cement layer and the number of cement layers are adopted as $0.5\mu m$ and 131, respectively. Figs. 9 and 10 show the voltage amplitude and average power changing with the load resistor. It is easily seen that the present theoretical results agree very well with the experimental data and the previous work for both the voltage amplitude and the average power when the loading frequency is 5 Hz. Fig. 9 also shows that the voltage amplitude tends to be the voltage amplitude of the open circuit with the increase of load resistor, and the open circuit voltage amplitude of the series model is N times that of the

parallel model. For a given load frequency, Fig. 10 shows that there is a matching load resistor to get a maximum average power, and the average power of the series model is same as that of the parallel model. Furthermore, the frequency of most civil engineering structures is between 0.1 Hz and 50 Hz (Li *et al.* 2001). Taking $q_0 = 1\text{MPa}$, the effects of the loading frequency on the matching load resistor and the maximum average power are shown in Figs. 11 and 12, respectively. It is found that the maximum average power and the matching load resistor of the series model are 1 time, N^2 times those of the parallel model, respectively. Additionally, with the increase of the loading frequency, the matching load resistor decreases, however, the maximum average power increases.

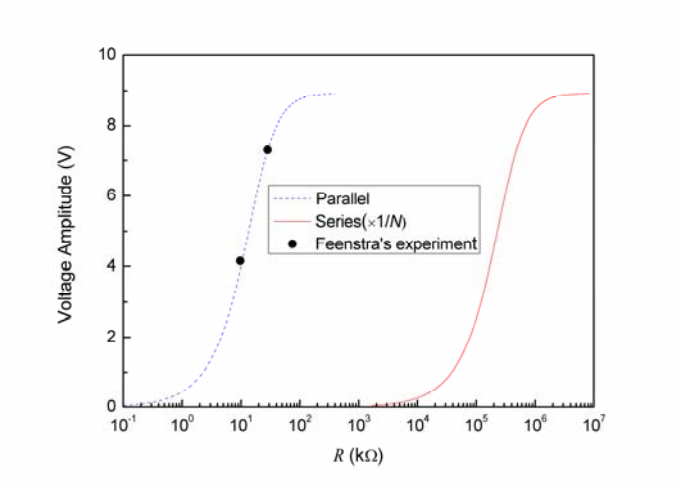

Fig. 9 The voltage amplitude changing with the load resistor *R*

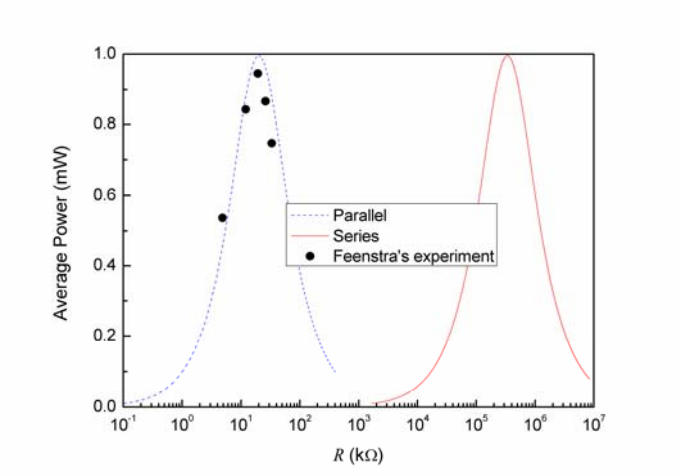

Fig. 10 The average power changing with the load resistor *R*

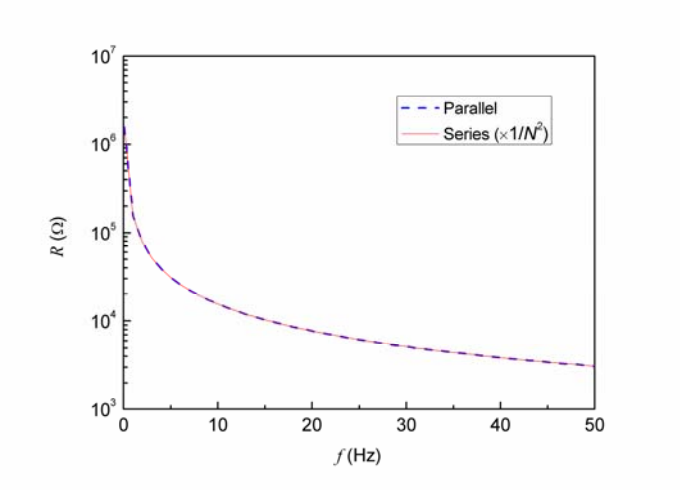

Fig. 11 The matching load resistor changing with the loading frequency

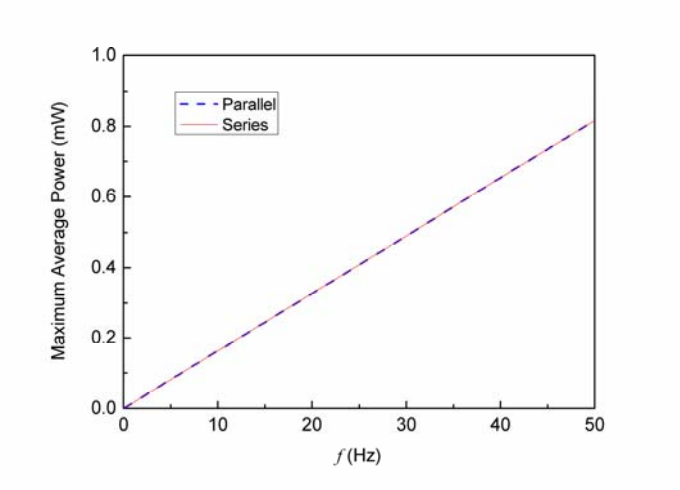

Fig. 12 The maximum average power changing with the loading frequency

Through the numerical analysis, the electromechanical properties of 2-2 cement-based piezoelectric transducers with different electrical conditions have been presented clearly. Based on the previous results, it is hoped that 2-2 cement-based piezoelectric transducers could be applied in many engineering fields. One is to monitor structural health in civil engineering. In this case, two kinds of transducers should be embedded in concrete structures as actuators and sensors, respectively. Actuators are used to generate waves through deformation and sensors are used to receive these waves and to output voltage signals. In order to obtain more deformation, the transducers in parallel electrically could be selected; in order to obtain more voltage signals, the transducers in series electrically could be selected. Another is to capture mechanical energy and

monitor train-running safety in railway system and traffic safety in road system. In the application of railway system, the transducers will be designed to prefabricate in concrete sleeper. On the one hand, they can convert mechanical energy into electrical energy for electricity needs along railway. On the other hand, they can be utilized in monitoring train-running safety through the relationship between output voltage signal and the real status of the train, such as speed, weight of axles, distances between two trains and so on. In addition, the similar application can also be used in road system through designing the transducers to embed in pavement. In above energy harvesting applications, the transducers in series electrically can generate greater voltage, but the other case can generate greater current. In practice, the different electrical conditions can be designed to meet various application purposes.

5. Conclusions

Based on the theory of piezo-elastic dynamics, the analytical solutions of 2-2 cement based piezoelectric transducers in series electrically are presented. The results can be drawn as follows.

- For the considered 2-2 cement based piezoelectric actuator, (a) both the resonance and anti-resonance frequencies of the series model are greater than those of the parallel model. (b) with the increase of the distance h_C between two adjacent piezoelectric layers, there exists only one maximum value in both resonance and anti-resonance curves for the parallel model, respectively; however, only one maximum value appears in anti-resonance curve for the series model; in addition, the resonance frequency is increased for the series model. (c) with the increase of the distance h_p between two adjacent cement layers, two kinds of models have the same characteristics that there exists only one minimum value in both resonance and anti-resonance curves, respectively. (d) the electrical connection has a little effect on the first electromechanical coupling factor.
- For the considered 2-2 cement based piezoelectric generator and for the frequency range in the field of civil engineering, (a) the maximum average power and the matching load resistor of the series model are 1 time and N^2 times those of the parallel model, respectively. (b) with the increase of the loading frequency, the matching load resistor decreases, but the maximum average power increases.
- The proposed 2-2 cement based piezoelectric transducers can be embedded in concrete structures to monitor structural health in civil engineering, prefabricated in concrete sleeper and pavement to convert mechanical energy into electrical energy for electricity needs along railway and road and monitor train-running safety in railway system and traffic safety in road system.

Acknowledgments

The research described in this paper was financially supported by the National Natural Science Foundation of China (51072018 and 51178040), and the Fundamental Research Funds for the Central Universities (2013JBM010).

References

Aizawa, S., Kakizawa, T. and Higasino, M. (1998), "Case studies of smart materials for civil structures", *Smart Mater. Struct.*, **7**(5), 617-626.

Bian, Z.G., Lim, C.W. and Chen, W.Q. (2006), "On functionally graded beams with integrated surface piezoelectric layers", *Compos. Struct.*, **72**(3), 339-351.

Carbonari, R.C., Silva, E.C.N. and Paulino, G.H. (2006), "Design of functionally graded piezoelectric actuators using topology optimization", *Proceedings of the 9th International Conference on Multiscale and Functionally Graded Materials*, Oahu, HI, USA, October.

Carbonari, R.C., Silva, E.C.N. and Paulino, G.H. (2007), "Topology optimization design of functionally graded bimorph-type piezoelectric actuators", *Smart Mater. Struct.*, **16**(6), 2605-2620.

Chaipanich, A. (2007), "Effect of PZT particle size on dielectric and piezoelectric properties of PZT–cement composites", *Curr. Appl. Phys.*, **7**(5), 574-577.

Dong, B.Q. and Li, Z.J. (2005), "Cement-based piezoelectric ceramic smart composites", *Compos. Sci. Technol.*, **65**(9), 1363-1371.

Feenstra, J., Granstrom, J. and Sodano, H.A. (2008), "Energy harvesting through a backpack employing a mechanically amplified piezoelectric stack", *Mech. Syst. Signal Pr.*, **22**(3), 721-734.

Flint, E.M., Liang, C. and Rogers, C.A. (1995), "Electromechanical analysis of piezoelectric stack active member power consumption", *J. Intel. Mat. Syst. Str.*, **6** (1), 117-124.

Han, R. and Shi, Z.F. (2011), "Exact analysis of 0-3 cement-based piezoelectric composites", *J. Intel. Mat. Syst. Str.*, **22**(3), 221-229.

Han, R. and Shi, Z.F. (2012), "Dynamic analysis of sandwich cement-based piezoelectric composites", *Compos. Sci. Technol.*, **72**(8), 894-901.

Han, R., Shi, Z.F. and Mo, Y.L. (2011), "Static analysis of 2-2 cement-based piezoelectric composites", *Arch. Appl. Mech.*, **81**(7), 839-851.

Huang, D.J., Ding, H.J. and Chen, W.Q. (2007), "Piezoelasticity solutions for functionally graded piezoelectric beams", *Smart Mater. Struct.*, **16**(3), 687-695.

Huang, D.J., Ding, H.J. and Chen, W.Q. (2008), "Analysis of functionally graded and laminated piezoelectric cantilever actuators subjected to constant voltage", *Smart Mater. Struct*., **17** (6), 065002.

Huston, D.R., Fuhr, P.L., Ambrose, T.P. and Barker, D.A. (1994), "Intelligent civil structures-activities in vermont", *Smart Mater. Struct.*, **3**(2), 129-139.

Jang, S., Sim, S.H., Jo, H. and Spencer Jr, B.F. (2012), "Full-scale experimental validation of decentralized damage identification using wireless smart sensors", *Smart Mater. Struct.*, **21**(11), 115019.

Jang, S., Jo, H., Cho, S., Mechitov, K., Rice, J.A., Sim, S.H., Jung, H.J., Yun, C.B., Spencer Jr, B.F. and Agha, G. (2010), "Structural health monitoring of a cable-stayed bridge using smart sensor technology: deployment and evaluation", *Smart Struct. Syst.*, **6**(5-6), 439-459.

Li, H.N., Li, D.S. and Song, G. (2004), "Recent applications of fiber optic sensors to health monitoring in civil engineering", *Eng. Struct.*, **26**(11), 1647-1657.

Li, P., Gu, H., Song, G., Zheng, R. and Mo, Y.L. (2010), "Concrete structural health monitoring using piezoceramic-based wireless sensor networks", *Smart Struct. Syst.*, **6**(5-6), 731-748.

Li, Y. and Shi, Z.F. (2009), "Free vibration of a functionally graded piezoelectric beam via state-space based differential quadrature", *Compos. Struct.*, **87**(3), 257-264.

Li, Z.J., Zhang, D. and Wu, K.R. (2001), "Cement matrix 2-2 piezoelectric composite—Part 1. Sensory effect", *Mater. Struct.*, **34** (8), 506-512.

Li, Z.J., Huang, S.F., Qin, L. and Cheng, X. (2007), "An investigation on 1–3 cement based piezoelectric composites", *Smart Mater. Struct.*, **16**, 999-1005.

Li, Z.X., Yang, X.M. and Li, Z. (2006), "Application of cement-based piezoelectric sensors for monitoring traffic flows", *J. Transp. Eng. - ASCE*, **132**(7), 565-573.

Lim, C.W., He, L.H. and Soh, A.K. (2001), "Three-dimensional electromechanical responses of a parallel piezoelectric bimorph", *Int. J. Solids Struct.*, **38**(16), 2833-2849.

Mason, W.P. (1950), *Piezoelectric crystals and their application to ultrasonics*, Van Nostrand Reinhold, New York, NY, USA.

Shi, Z.F. and Wang, J.J. (2013), "Dynamic analysis of 2-2 cement-based piezoelectric transducers", *J. Intel. Mat. Syst. Str.*, **24**(1), 99-107.

Song, G., Mo, Y.L., Otero, K. and Gu, H. (2006), "Health monitoring and rehabilitation of a concrete structure using intelligent materials", *Smart Mater. Struct.*, **15**(2), 309-314.

Song, G., Gu, H., Mo, Y.L., Hsu, T.T.C. and Dhonde, H. (2007), "Concrete structural health monitoring using embedded piezoceramic transducers", *Smart Mater. Struct.*, **16**(4), 959-968.

Xiang, H.J. and Shi, Z.F. (2008), "Static analysis for multi-layered piezoelectric cantilevers", *Int. J. Solids Struct.*, **45**(1), 113-128.

Xiang, H.J. and Shi, Z.F. (2009), "Static analysis of a multilayer piezoelectric actuator with bonding layers and electrodes", *Smart Struct. Syst.*, **5**(5), 547-564.

Xu, D.Y., Cheng, X., Huang, S.F. and Jiang, M.H. (2009), "Electromechanical Properties of 2-2 Cement Based Piezoelectric Composite", *Curr. Appl. Phys.*, **9** (4), 816-819.

Xu, D.Y., Cheng, X., Huang, S.F. and Jiang, M.H. (2011), "Effect of cement matrix and composite thickness on properties of 2-2 type cement-based piezoelectric composites", *J. Compos. Mater.*, **45**(20), 2083-2089.

Yang, J. and Xiang, H.J. (2007), "Thermo-electro-mechanical characteristics of functionally graded piezoelectric actuators", *Smart Mater. Struct.*, **16**(3), 784-797.

Yang, J., Kitipornchai, S. and Liew, K.M. (2004), "Non-linear analysis of the thermo-electro-mechanical behaviour of shear deformable FGM plates with piezoelectric actuators", *Int. J. Numer. Meth. Eng.*, **59** (12), 1605-1632.

Yao, R.X. and Shi, Z.F. (2011), "Steady-state forced vibration of functionally graded piezoelectric beams", *J. Intel. Mat. Syst. Str.*, **22** (8), 769-779.

Zhang, D., Li, Z.J. and Wu, K.R. (2002), "2-2 piezoelectric cement matrix composite: Part II. Actuator effect", *Cement Concrete Res.*, **32** (5), 825-830.

Zhang, T.T. and Shi, Z.F. (2006), "Two-dimensional exact analysis for piezoelectric curved actuators", *J. Micromech. Microeng.*, **16** (3), 640-647.

Zhang, T.T. and Shi, Z.F. (2011), "Exact analysis of the dynamic properties of a 2–2 cement based piezoelectric transducer", *Smart Mater. Struct.*, **20** (8), 085017.

BF

Appendix A.

$$\begin{cases} A_{Ci} = \delta_i^1 A_{C1} + \lambda_i^1 C_{11} \\ B_{Ci} = \delta_i^2 A_{C1} + \lambda_i^2 C_{11} \end{cases} \tag{A.1}$$

$$\begin{cases} A_{Pi} = \delta_i^3 A_{C1} + \lambda_i^3 C_{11} \\ B_{Pi} = \delta_i^4 A_{C1} + \lambda_i^4 C_{11} \end{cases} \tag{A.2}$$

$$C_{1i} = \alpha_i C_{11} \tag{A.3}$$

$$\begin{cases} C_{01} = \delta_{01} A_{C1} + \lambda_{01} C_{11} \\ C_{0i} = \delta_i^8 A_{C1} + \lambda_i^8 C_{11} (i = 2,3,\cdots,N) \end{cases} \tag{A.4}$$

where

$$\begin{cases} \delta_1^1 = 1 \\ \delta_1^2 = 0 \\ \delta_{i+1}^1 = a_i^5 \delta_i^1 + b_i^5 \delta_i^2 \\ \delta_{i+1}^2 = a_i^6 \delta_i^1 + b_i^6 \delta_i^2 \end{cases} \tag{A.5}$$

$$\begin{cases} \lambda_1^1 = 0 \\ \lambda_1^2 = 0 \\ \lambda_{i+1}^1 = a_i^5 \lambda_i^1 + b_i^5 \lambda_i^2 + \alpha_i c_i^1 \\ \lambda_{i+1}^2 = a_i^6 \lambda_i^1 + b_i^6 \lambda_i^2 + \alpha_i c_i^2 \end{cases} \tag{A.6}$$

$$\begin{cases} \delta_i^3 = a_i^1 \delta_i^1 + b_i^1 \delta_i^2 \\ \delta_i^4 = a_i^2 \delta_i^1 + b_i^2 \delta_i^2 \\ \lambda_i^3 = a_i^1 \lambda_i^1 + b_i^1 \lambda_i^2 - a\alpha_i \cos k_P h_{2i-1} \\ \lambda_i^4 = a_i^2 \lambda_i^1 + b_i^2 \lambda_i^2 + a\alpha_i \sin k_P h_{2i-1} \end{cases} \tag{A.7}$$

$$\begin{cases} \delta_i^5 = \delta_i^6 - \delta_i^7 \\ \lambda_i^5 = \lambda_i^6 - \lambda_i^7 \end{cases} \tag{A.8}$$

$$\begin{cases} \delta_i^6 = \delta_i^3 \sin k_P h_{2i} + \delta_i^4 \cos k_P h_{2i} \\ \delta_i^7 = \delta_{i+1}^3 \sin k_P h_{2i+1} + \delta_{i+1}^4 \cos k_P h_{2i+1} \\ \lambda_i^6 = \lambda_i^3 \sin k_P h_{2i} + \lambda_i^4 \cos k_P h_{2i} + \alpha_i h_{2i} \\ \lambda_i^7 = \lambda_{i+1}^3 \sin k_P h_{2i+1} + \lambda_{i+1}^4 \cos k_P h_{2i+1} + \alpha_{i+1} h_{2i+1} \end{cases} \tag{A.9}$$

$$\begin{cases} \delta_i^8 = \delta_{01} + \sum_{k=1}^{i-1} \delta_k^5 \\ \lambda_i^8 = \lambda_{01} + \sum_{k=1}^{i-1} \lambda_k^5 \end{cases} (i = 2, 3, \cdots, N) \tag{A.10}$$

$$\begin{cases} a = \dfrac{e_{33}^2}{p_P \kappa_{33}^{\varepsilon}} \\ \alpha_i = 1 \\ \delta_{01} = -(\delta_1^3 \sin k_P h_1 + \delta_1^4 \cos k_P h_1) \\ \lambda_{01} = -(\lambda_1^3 \sin k_P h_1 + \lambda_1^4 \cos k_P h_1 + h_1) \end{cases} \tag{A.11}$$

$$\begin{cases} a_i^1 = \sin k_C h_{2i-1} \sin k_P h_{2i-1} + \dfrac{p_C}{p_P} \cos k_C h_{2i-1} \cos k_P h_{2i-1} \\ b_i^1 = \cos k_C h_{2i-1} \sin k_P h_{2i-1} - \dfrac{p_C}{p_P} \sin k_C h_{2i-1} \cos k_P h_{2i-1} \\ a_i^2 = \sin k_C h_{2i-1} \cos k_P h_{2i-1} - \dfrac{p_C}{p_P} \cos k_C h_{2i-1} \sin k_P h_{2i-1} \\ b_i^2 = \cos k_C h_{2i-1} \cos k_P h_{2i-1} + \dfrac{p_C}{p_P} \sin k_C h_{2i-1} \sin k_P h_{2i-1} \end{cases} \tag{A.12}$$

$$\begin{cases} a_i^3 = \sin k_C h_{2i} \sin k_P h_{2i} + \dfrac{p_C}{p_P} \cos k_C h_{2i} \cos k_P h_{2i} \\ b_i^3 = \cos k_C h_{2i} \sin k_P h_{2i} - \dfrac{p_C}{p_P} \sin k_C h_{2i} \cos k_P h_{2i} \\ a_i^4 = \sin k_C h_{2i} \cos k_P h_{2i} - \dfrac{p_C}{p_P} \cos k_C h_{2i} \sin k_P h_{2i} \\ b_i^4 = \cos k_C h_{2i} \cos k_P h_{2i} + \dfrac{p_C}{p_P} \sin k_C h_{2i} \sin k_P h_{2i} \end{cases} \tag{A.13}$$

$$\begin{cases} H_i^1 = a_i^3 b_i^4 - a_i^4 b_i^3 \\ a_i^5 = (b_i^4 a_i^1 - b_i^3 a_i^2)/H_i^1 \\ b_i^5 = (b_i^4 b_i^1 - b_i^3 b_i^2)/H_i^1 \\ c_i^1 = [ab_i^4(\cos k_P h_{2i} - \cos k_P h_{2i-1}) - ab_i^3(\sin k_P h_{2i-1} - \sin k_P h_{2i})]/H_i^1 \\ a_i^6 = -(a_i^4 a_i^1 - a_i^3 a_i^2)/H_i^1 \\ b_i^6 = -(a_i^4 b_i^1 - a_i^3 b_i^2)/H_i^1 \\ c_i^2 = -[aa_i^4(\cos k_P h_{2i} - \cos k_P h_{2i-1}) - aa_i^3(\sin k_P h_{2i-1} - \sin k_P h_{2i})]/H_i^1 \end{cases} \tag{A.14}$$